Supporting Information

Development of a New Type of Multi-Functional Mechanochromic Luminescence Materials by Infusing a Phenyl Rotator into the Structure of 3,4-diphenylmaleic anhydride

Zexin Wang [a, b], Liwei Chen [b], Xiang Lin [b], Wei Liu [b], Jun Han [c], Nannan Chen [b], Hong Jiang [b], Shitao Sun [a], Zhenli Li [a], Jinle Hao [a], Bin Lin [a], Renfu Li [d], Xueyuan Chen [d], Xin Zhai *, [a], and Lijun Xie*, [b]

[a] Key Laboratory of Structure-based Drug Design and Discovery, Ministry of Education, School of Pharmaceutical Engineering, Shenyang Pharmaceutical University. Shenyang, Liaoning 110016, P. R. China

[b] Fujian Provincial Key Laboratory of Screening for Novel Microbial Products, Fujian Institute of Microbiology, Fuzhou, Fujian 350007, P. R. China

[c] Department of Physics, Southern University of Science and Technology, Huiyuan Bldg 1, 1088 Xueyuan Blvd, Nanshan, Shenzhen 518055, P. R. China

[d] CAS Key Laboratory of Design and Assembly of Functional Nanostructures, and Fujian Key Laboratory of Nanomaterials, Fujian Institute of Research on the Structure of Matter, Chinese Academy of Sciences, Fuzhou, Fujian 350002, P.R. China

Table of Contents

Section	Title	Page
Figure S1-S21	Characterization of compounds	S3
Figure S22	Solvatochromism of **W1**, **W4** and **W6**	S13
Table S1	The photophysical data of **W1**, **W4** and **W6** in different solvents	S14
Figure S23	Aggregation-induced emission of **W1**, **W4** and **W6**	S15
Table S2	Solid state fluorescence QY of **W1, W4** and **W6**	S15
Figure S24	The normalized PL intensity of crystals **W6R** and **W6Y**	S16
Figure S25-27	Molecular conformation of **W1, W6R** and **W6Y**	S16
Figure S28	The ORTEP plot of **W6R** and **W6Y**	S18
Table S3-S5	Crystal data and structure refinement for **W1, W6R** and **W6Y**	S19
Figure S29, S30	Mechanochromic luminescence of **W4** and **W6**	S22
Figure S31	Differential scanning calorimetry of **W4** and **W6**	S24
Figure S32	Sensing properties toward protonic acids of **W6**	S24
Figure S33	Vapochromism of **W1**	S25

Characterization of W1

Synthesis of W1. (General procedure) Piperidine, 3 drops, was added to a mixture of 0.140 g (0.0004 mol) of intermediate (**W**) and 0.140 g of 2-Morpholinobezaldehyde in 10 ml of MeOH, and the mixture was stirred at room temperature for 12 h in dark atmosphere. The mixture was then cooled, and the precipitate was filtered off and washed with MeOH. The yellow powder (**W1**, 0.13 g) was obtained with the yield 92%. ^{1}H NMR (600 MHz, DMSO-d_6) δ 8.14 (d, J = 8.3 Hz, 2H), 8.05 (d, J = 7.8 Hz, 1H), 7.74 (d, J = 8.3 Hz, 2H), 7.37 (t, J = 8.3 Hz, 1H), 7.30 (d, J = 8.1 Hz, 2H), 7.23 – 7.14 (m, 3H), 7.12 (d, J = 8.0 Hz, 1H), 6.21 (s, 1H), 3.47 (s, 4H), 2.81 (t, J = 4.3 Hz, 4H), 2.29 (s, 3H). ^{13}C NMR (151 MHz, DMSO-d_6) δ 168.2, 152.4, 149.0, 147.9, 142.1, 139.3, 136.2, 131.0, 130.8, 130.7, 129.6, 129.2, 128.1, 126.6, 126.3, 125.2, 123.8, 119.7, 109.1, 66.8, 53.1, 43.8, 21.3. HRMS (ESI): calced for $C_{29}H_{27}NO_5S$: 502.1683 ([M+H]+), found:502.1687.

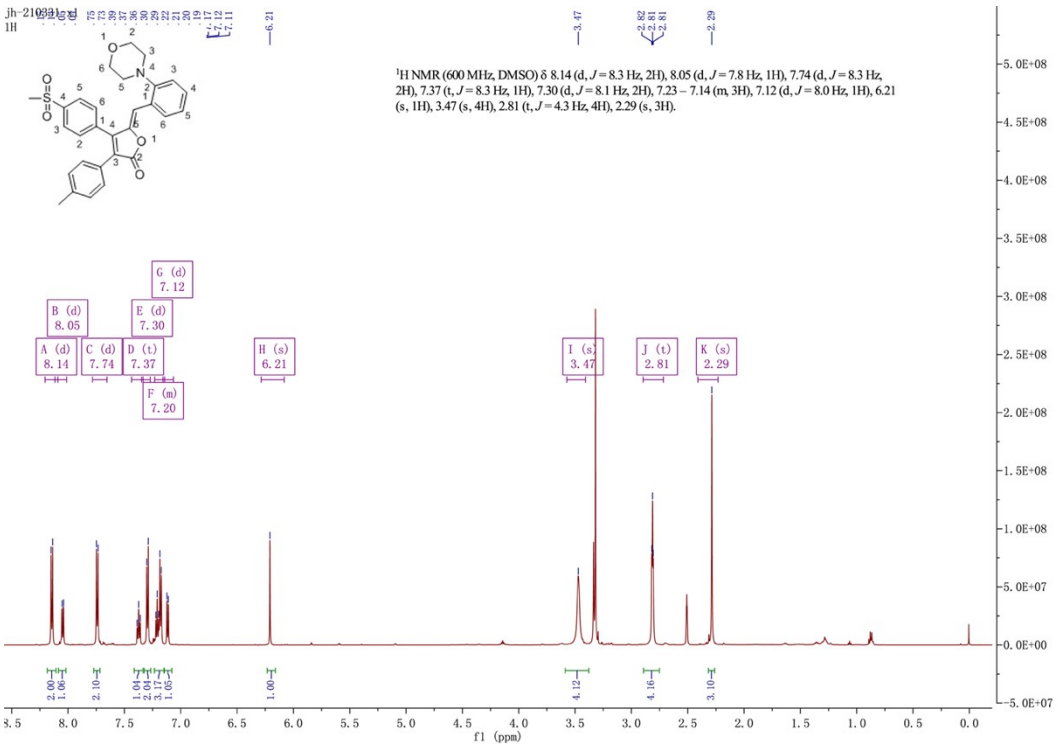

Figure S1. ^{1}H NMR spectrum of **W1** in DMSO-d_6 (600 MHz, 298K).

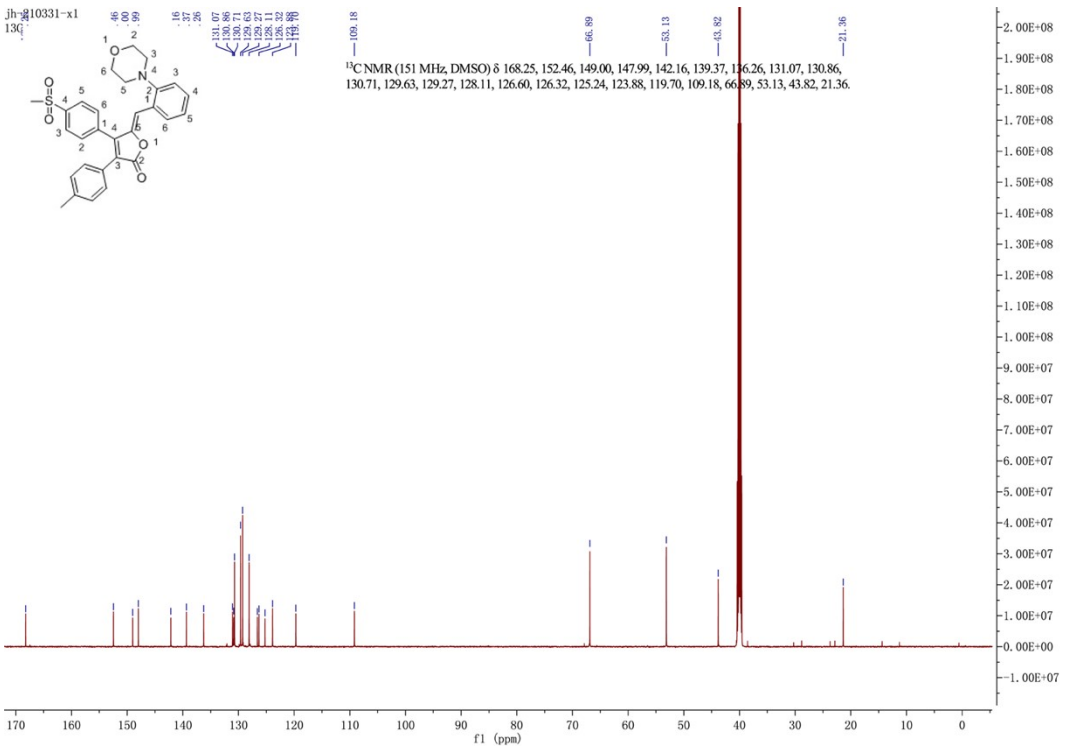

Figure S2. ^{13}C NMR spectrum of **W1** in DMSO-d_6 (151 MHz, 298K).

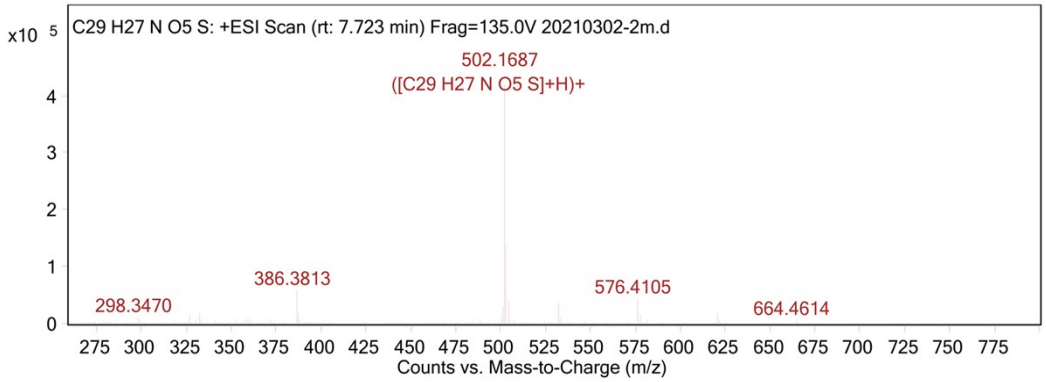

Figure S3. HRMS spectrum of **W1**

Characterization of W2

Synthesis of W2. The orange-red powder (**W2**, 0.12 g) was synthesized following the the general procedure with the yield 83%. ^{1}H NMR (600 MHz, DMSO-d_6) δ 8.06 (d, J = 8.1 Hz, 2H), 7.71 (d, J = 8.7 Hz, 2H), 7.67 (d, J = 8.1 Hz, 2H), 7.21 (d, J = 8.0 Hz, 2H), 7.14 (d, J = 7.9 Hz, 2H), 7.01 (d, J = 8.7 Hz, 2H), 5.97 (s, 1H), 3.73 (s, 4H), 3.34 (s, 3H), 3.25 (s, 4H), 2.28 (s, 3H). ^{13}C NMR (151 MHz, DMSO-d_6) δ 168.2, 151.7, 148.6, 145.4, 141.9, 138.8, 135.9, 132.5, 130.7, 129.4, 129.30, 128.0, 126.7, 123.8, 123.5, 114.6, 114.0, 66.3, 47.4, 43.7, 21.3. HRMS (ESI): calced for $C_{29}H_{27}NO_5S$: 502.1683 ([M+H]+), found:502.1688.

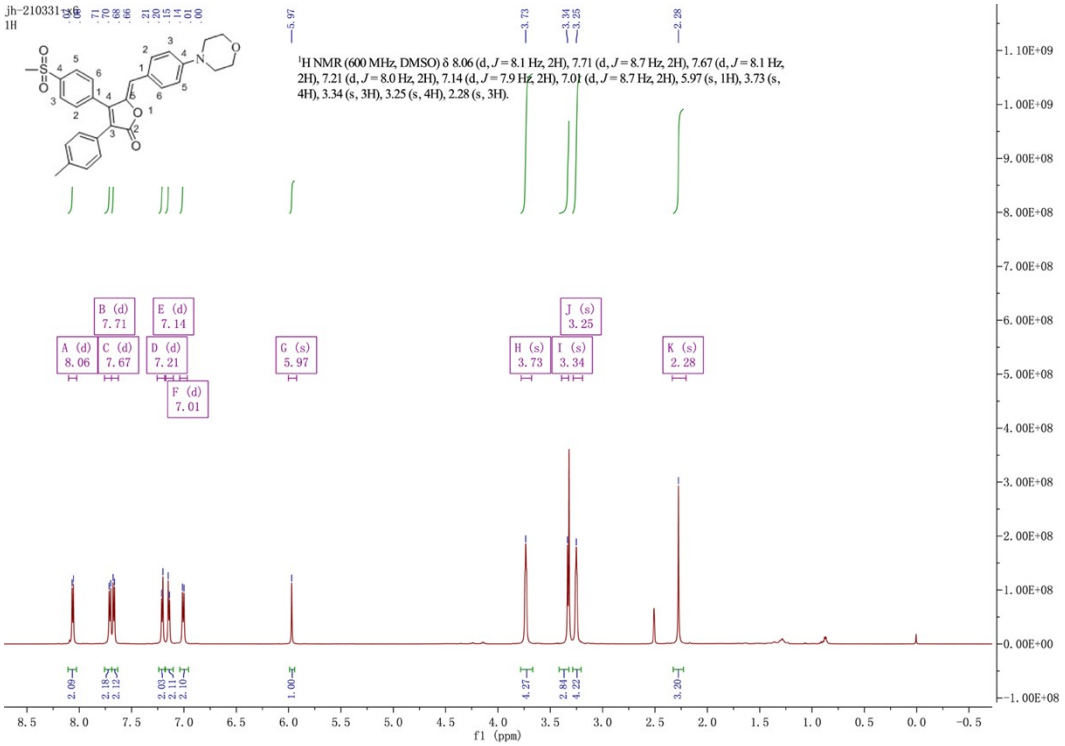

Figure S4. ^{1}H NMR spectrum of **W2** in DMSO-d_6 (600 MHz, 298K).

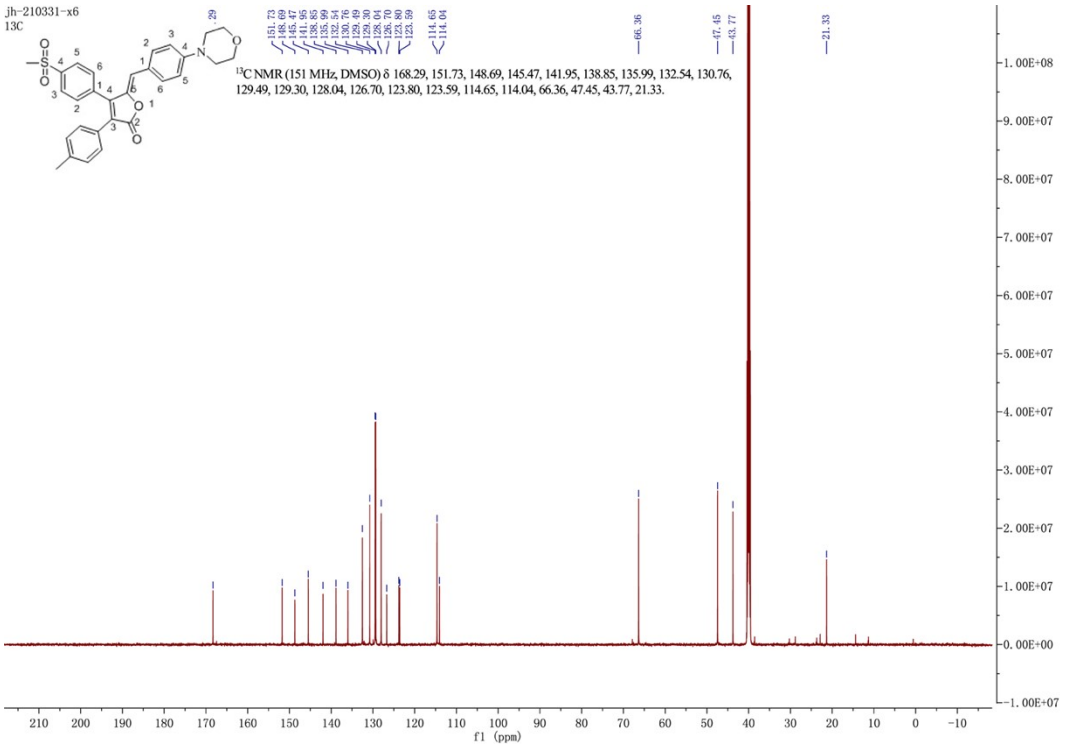

Figure S5. ^{13}C NMR spectrum of **W2** in DMSO-d_6 (151 MHz, 298K).

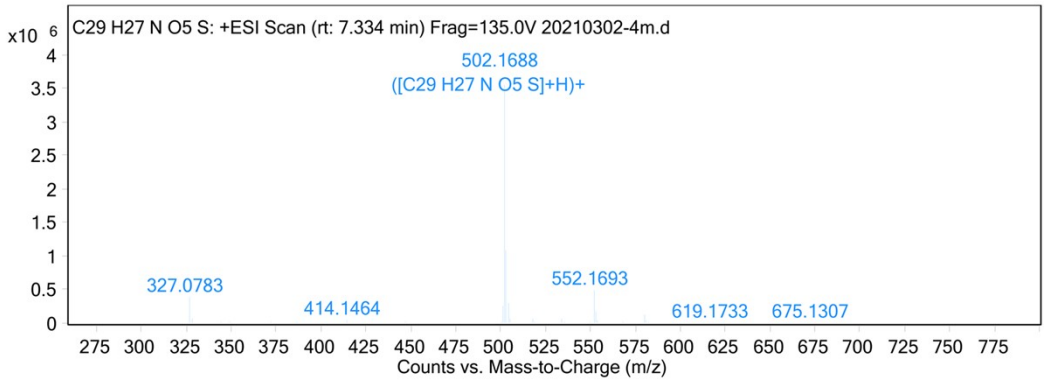

Figure S6. HRMS spectrum of **W2**

Characterization of W3

Synthesis of W3. The red powder (**W3**, 0.10 g) was synthesized following the general procedure with the yield 72% ^{1}H NMR (600 MHz, DMSO-d_6) δ 8.06 (d, J = 8.2 Hz, 2H), 7.68 (t, J = 8.8 Hz, 4H), 7.21 (d, J = 8.1 Hz, 2H), 7.14 (d, J = 8.1 Hz, 2H), 6.99 (d, J = 8.9 Hz, 2H), 5.96 (s, 1H), 3.28-3.38 (m, 4H), 2.44 (s, 4H), 2.28 (s, 3H), 2.22 (s, 3H). ^{13}C NMR (151 MHz, DMSO-d_6) δ 168.3, 151.6, 148.6, 145.3, 141.9, 138.8, 136.0, 132.5, 130.7, 129.4, 129.2, 128.0, 126.7, 123.6, 123.1, 114.7, 114.1, 54.8, 47.0, 46.1, 43.7, 21.3. HRMS (ESI): calced for $C_{30}H_{30}N_2O_4S$: 515.1999 ([M+H]+), found:515.1998.

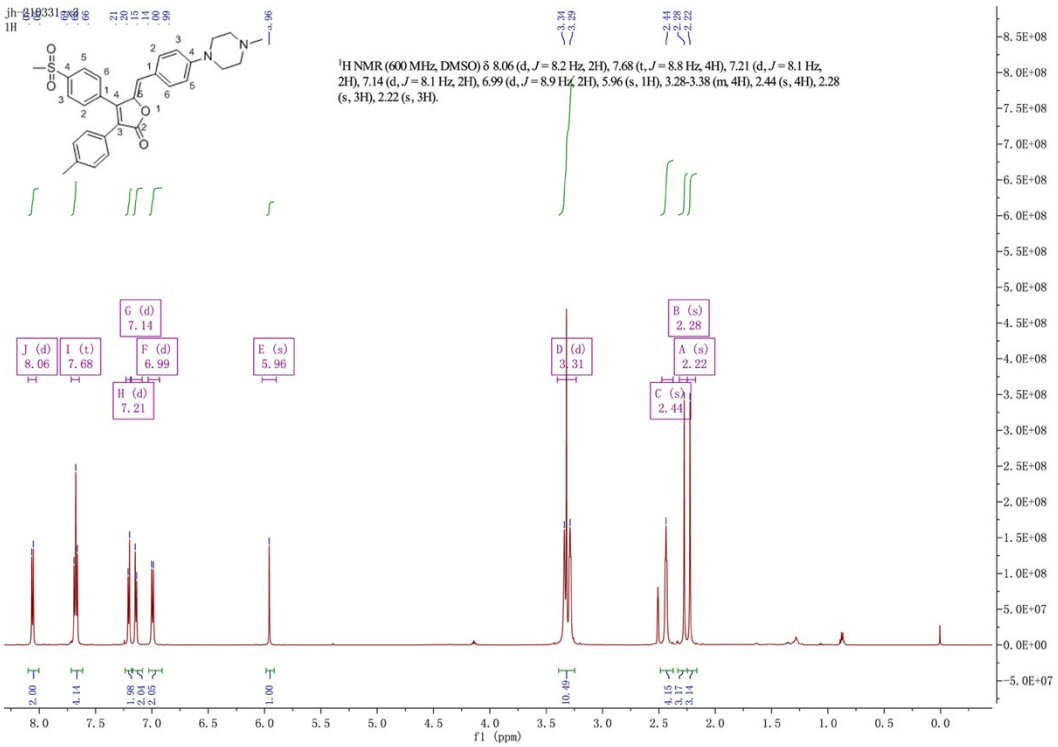

Figure S7. ^{1}H NMR spectrum of **W3** in DMSO-d_6 (600 MHz, 298K).

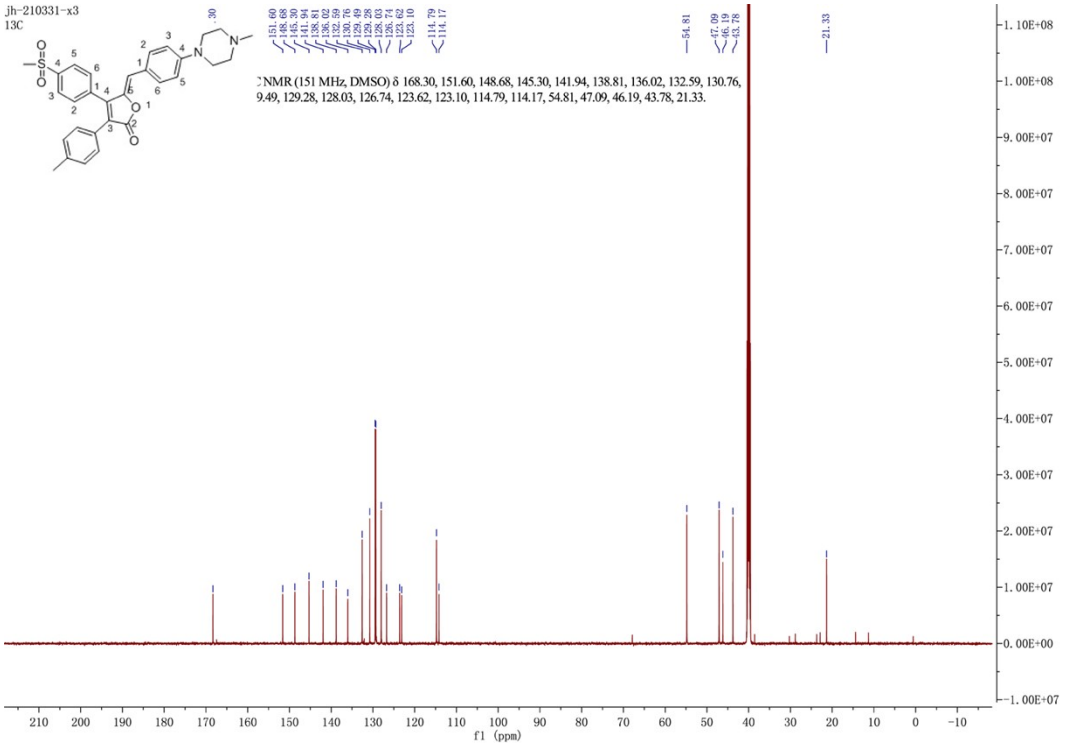

Figure S8. ^{13}C NMR spectrum of **W3** in DMSO-d_6 (151 MHz, 298K).

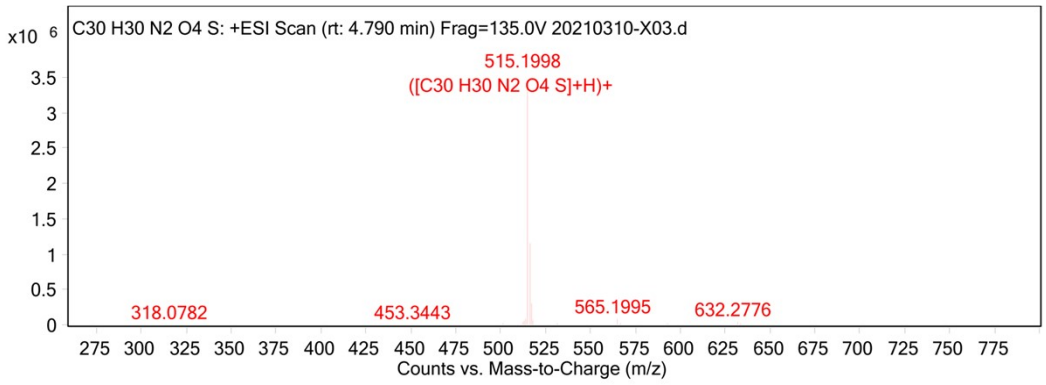

Figure S9. HRMS spectrum of **W3**

Characterization of W4

Synthesis of W4. The orange powder (**W4**, 0.12 g) was synthesized following the general procedure with the yield 88%. ^{1}H NMR (600MHz, DMSO-d_6) δ 8.07 (d,J = 8.4Hz, 2H), 7.75 – 7.66 (m, 5H), 7.40 – 7.34 (m, 4H), 7.21 (d,J = 8.2Hz, 2H), 7.18 – 7.14 (m, 4H), 7.11 (d,J = 7.5Hz, 2H), 6.93 (d,J = 8.9Hz, 2H), 5.99 (s, 1H), 2.28 (s, 3H). ^{13}C NMR(151MHz, DMSO-d_6) δ 168.1, 148.7, 148.6, 146.6, 146.3, 142.0, 139.0, 135.8, 132.4, 132.1, 132.0, 130.7, 130.2, 129.5, 129.3, 129.1, 128.0, 126.5, 126.4, 125.7, 124.8, 124.5, 121.2, 113.2, 67.8, 43.7, 30.2, 28.8. HRMS (ESI): calced for $C_{37}H_{29}NO_4S$: 584.1890 ([M+H]+), found:584.1881.

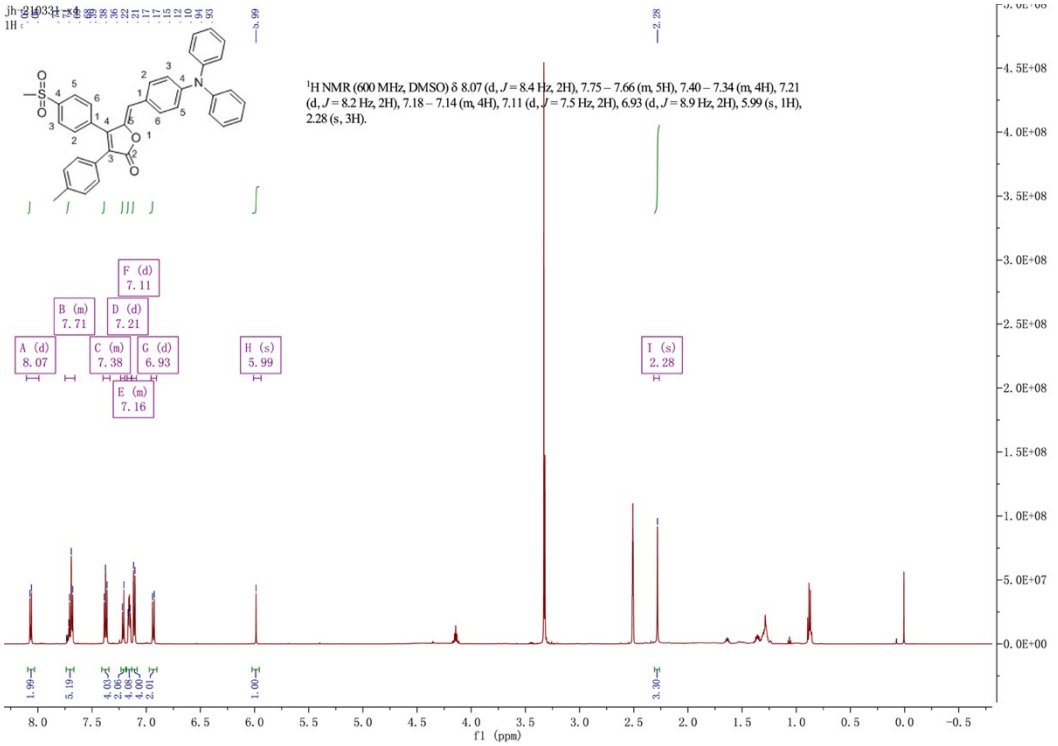

Figure S10. ^{1}H NMR spectrum of **W4** in DMSO-d_6 (600 MHz, 298K).

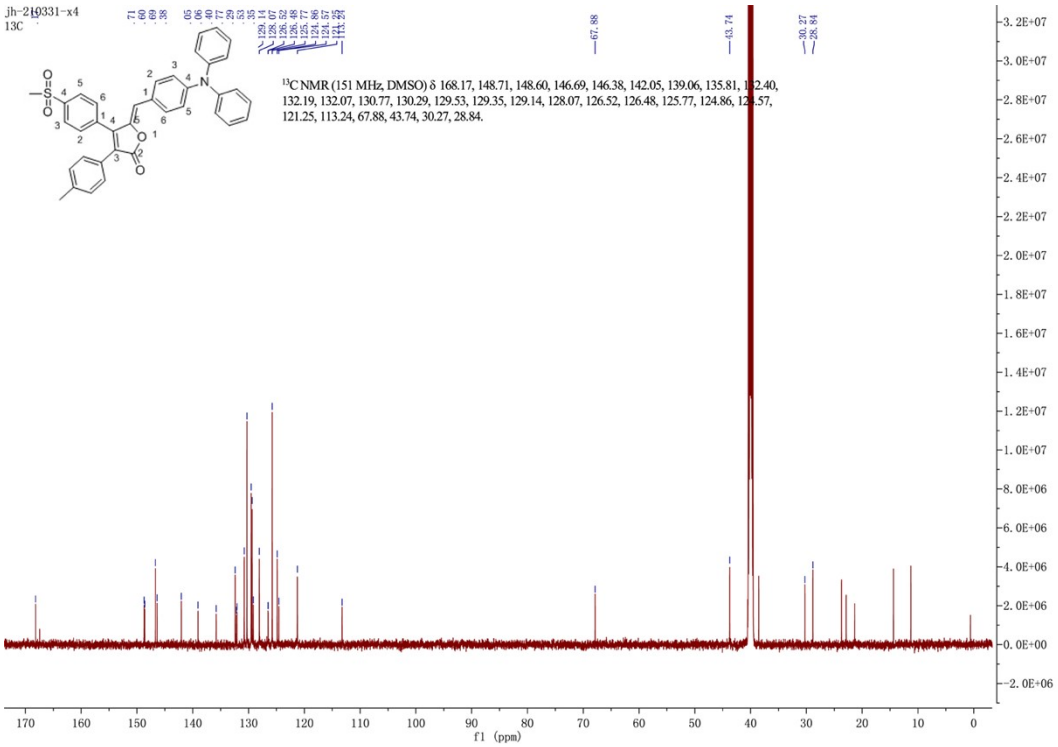

Figure S11. ^{13}C NMR spectrum of **W4** in DMSO-d_6 (151MHz, 298K).

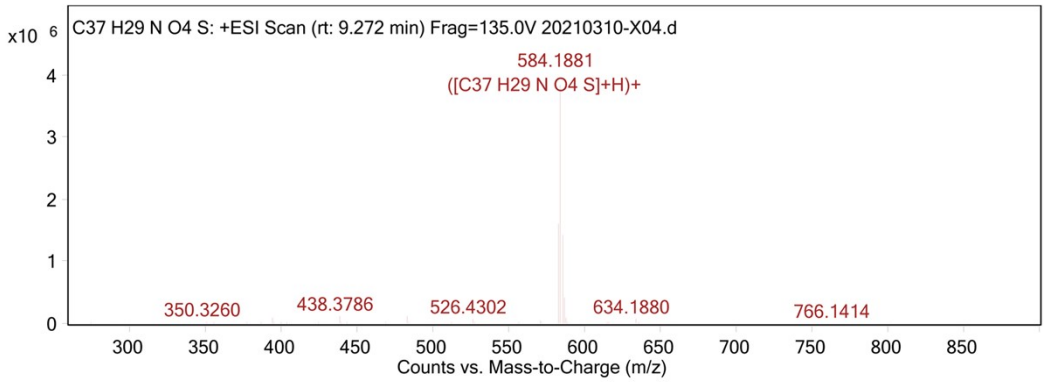

Figure S12. HRMS spectrum of **W4**

Characterization of W5

Synthesis of W5. The red powder (**W5**, 0.12 g) was synthesized following the general procedure with the yield 88%. ^{1}H NMR (600 MHz, DMSO-d_6) δ 8.06 (d, J = 8.2 Hz, 2H), 7.76 – 7.53 (m, 4H), 7.20 (d, J = 8.0 Hz, 2H), 7.14 (d, J = 8.0 Hz, 2H), 6.77 (d, J = 8.9 Hz, 1H), 5.95 (s, 1H), 3.32 (s, 3H), 3.01 (s, 6H), 2.27 (s, 3H). ^{13}C NMR (151 MHz, DMSO-d_6) δ 168.3, 151.2, 148.6, 144.5, 141.8, 138.6, 136.1, 132.8, 130.7, 129.4, 129.2, 128.0, 126.9, 122.8, 120.9, 114.8, 112.4, 67.8, 43.7, 30.2, 28.8, 21.3. HRMS (ESI): calced for $C_{27}H_{25}NO_4S$: 460.1577 ([M+H]+), found:460.1612.

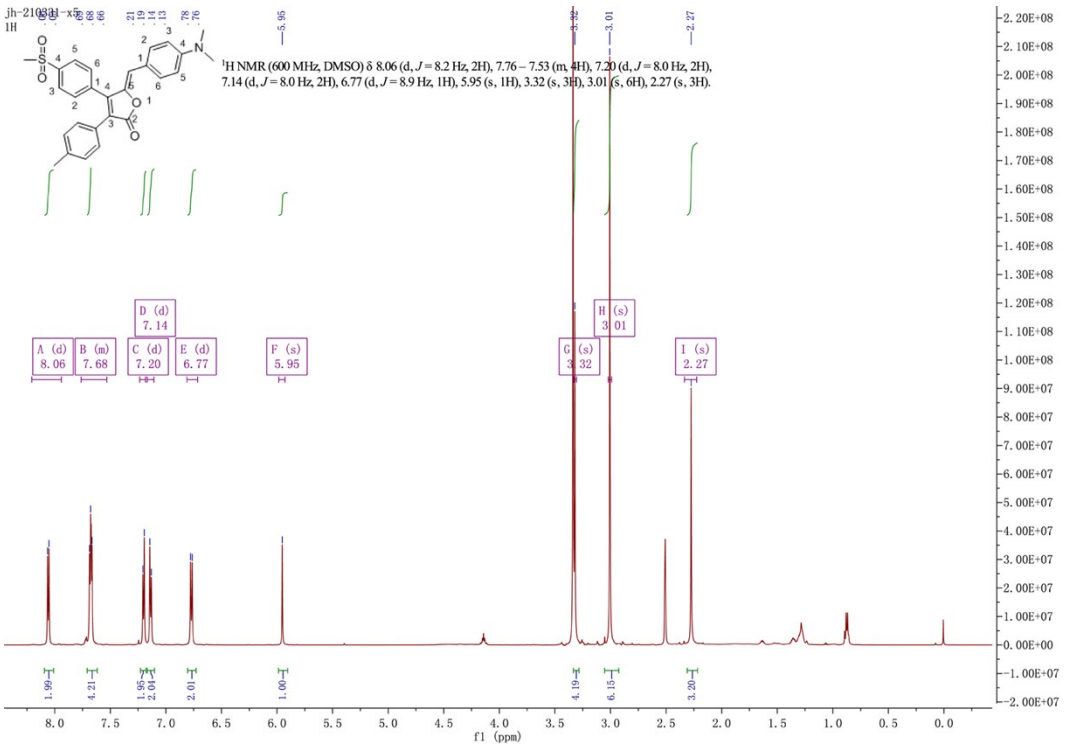

Figure S13. ^{1}H NMR spectrum of **W5** in DMSO-d_6 (600 MHz, 298K).

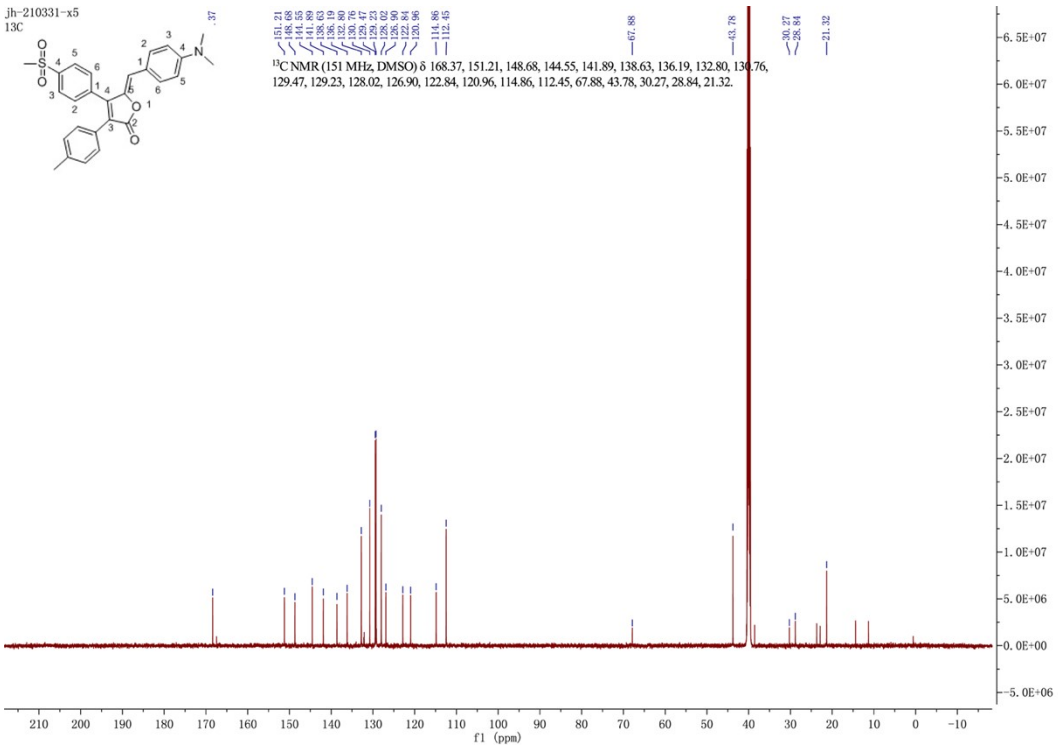

Figure S14. ^{13}C NMR spectrum of **W5** in DMSO-d_6 (151 MHz, 298K).

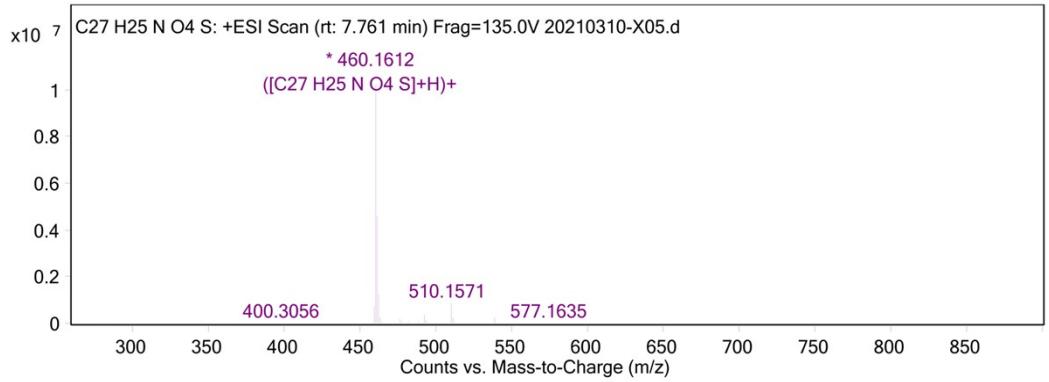

Figure S15. HRMS spectrum of **W5**

Characterization of W6

Synthesis of W6. The orange powder (**W6**, 0.12 g) was synthesized following the general procedure with the yield 83%. ^{1}H NMR (600 MHz, DMSO-d_6) δ 8.12 (d, J = 8.3 Hz, 2H), 8.05 (d, J = 9.1 Hz, 1H), 7.75 (d, J = 8.3 Hz, 2H), 7.34 (t, J = 7.0 Hz, 1H), 7.30 (d, J = 8.1 Hz, 2H), 7.17 (dd, J = 15.5, 7.9 Hz, 3H), 7.08 (d, J = 7.8 Hz, 1H), 6.21 (s, 1H), 3.30 (s, 3H), 2.74 (s, 4H), 2.29 (s, 3H), 1.45 – 1.22 (m, 6H). ^{13}C NMR (151 MHz, DMSO-d_6) δ 168.2, 153.8, 149.1, 147.7, 142.1, 139.3, 136.2, 130.9, 130.7, 129.6, 129.2, 128.0, 126.6, 126.3, 125.0, 123.3, 119.8,

109.5, 56.5, 54.1, 43.8, 26.3, 23.9, 21.3, 19.0. HRMS (ESI): calced for $C_{30}H_{29}NO_4S$: 500.1890 ([M+H]+), found:500.1884.

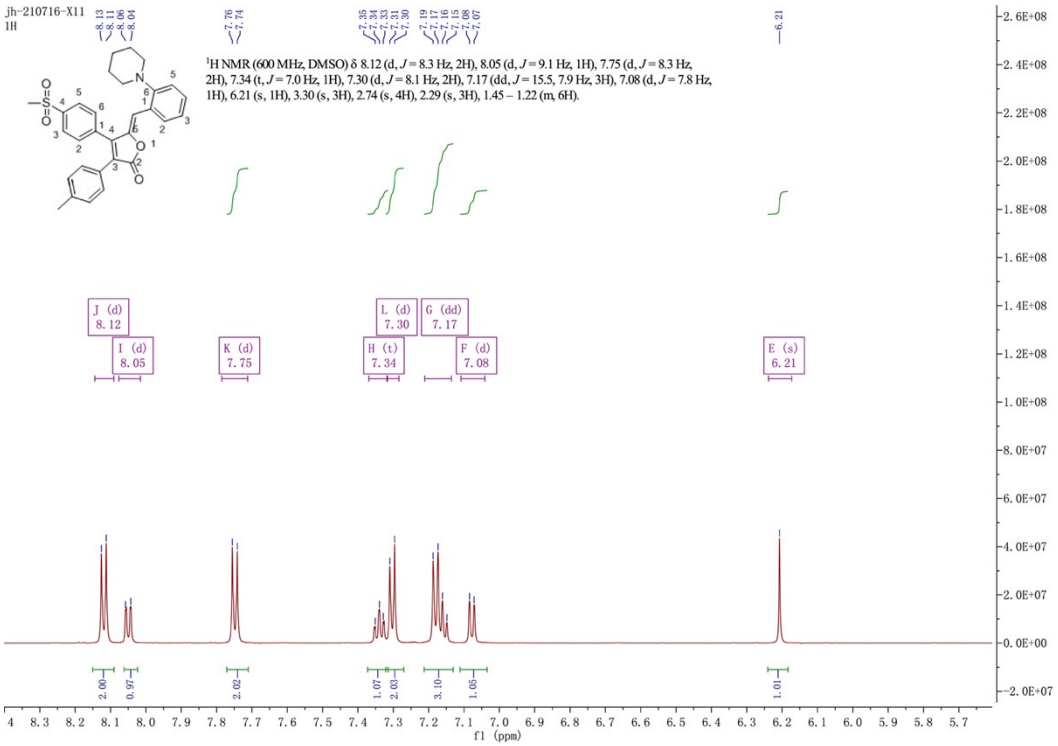

Figure S16. ^{1}H NMR spectrum of **W6** in DMSO-d_6 (600 MHz, 298K).

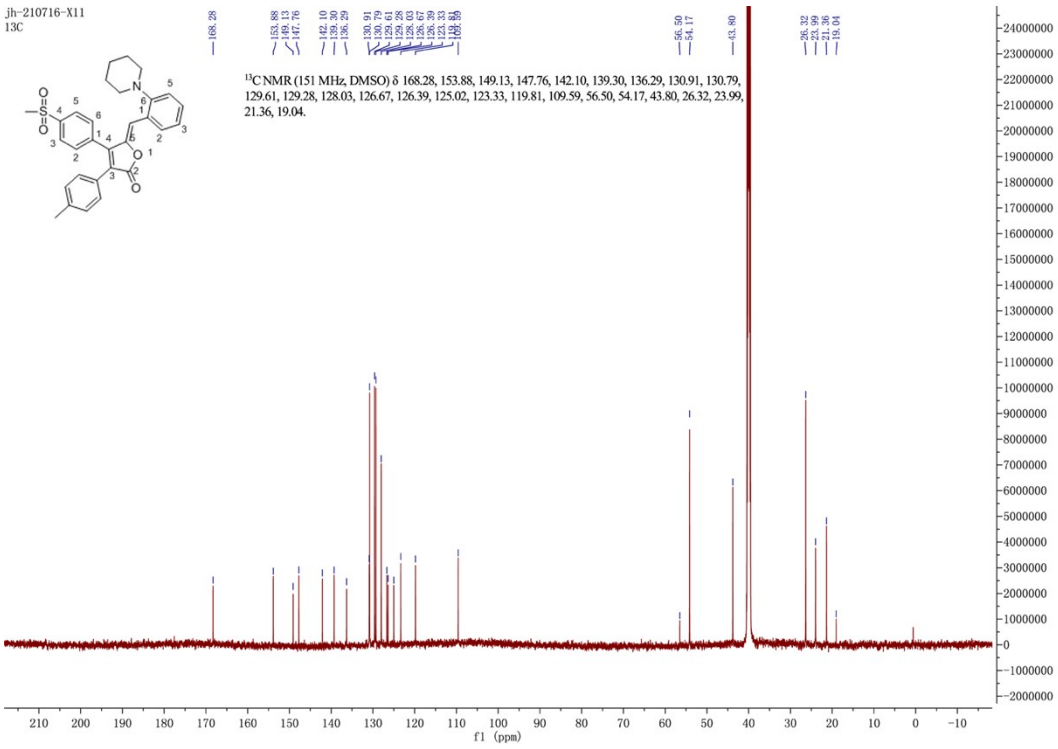

Figure S17. ^{13}C NMR spectrum of **W6** in DMSO-d_6 (151 MHz, 298K).

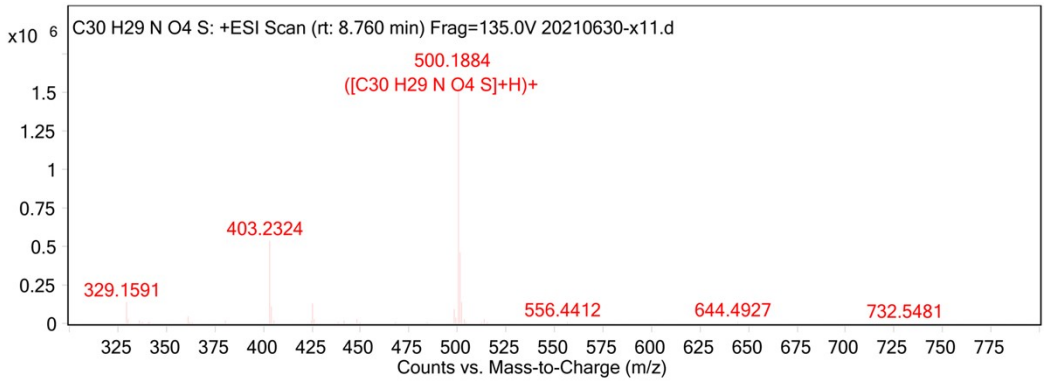

Figure S18. HRMS spectrum of **W6**

Characterization of W7

Synthesis of W7. The red powder (**W7**, 0.12 g) was synthesized following the general procedure with the yield 85%. ^{1}H NMR (600 MHz, DMSO-d_6) δ 8.06 (d, J = 8.2 Hz, 2H), 7.66 (d, J = 8.4 Hz, 4H), 7.20 (d, J = 8.1 Hz, 2H), 7.14 (d, J = 8.1 Hz, 2H), 6.97 (d, J = 9.0 Hz, 2H), 5.95 (s, 1H), 3.34 (s, 3H), 2.27 (s, 4H), 1.59 (s, 6H). ^{13}C NMR (151 MHz, DMSO-d_6) δ 168.3, 151.7, 148.6, 145.0, 141.9, 138.7, 136.0, 132.7, 130.7, 129.4, 129.2, 128.0, 126.8, 123.2, 122.3, 114.7, 114.3, 48.3, 43.7, 25.4, 24.4, 21.3. HRMS (ESI): calced for $C_{30}H_{29}NO_4S$: 500.1890 ([M+H]+), found:500.1887.

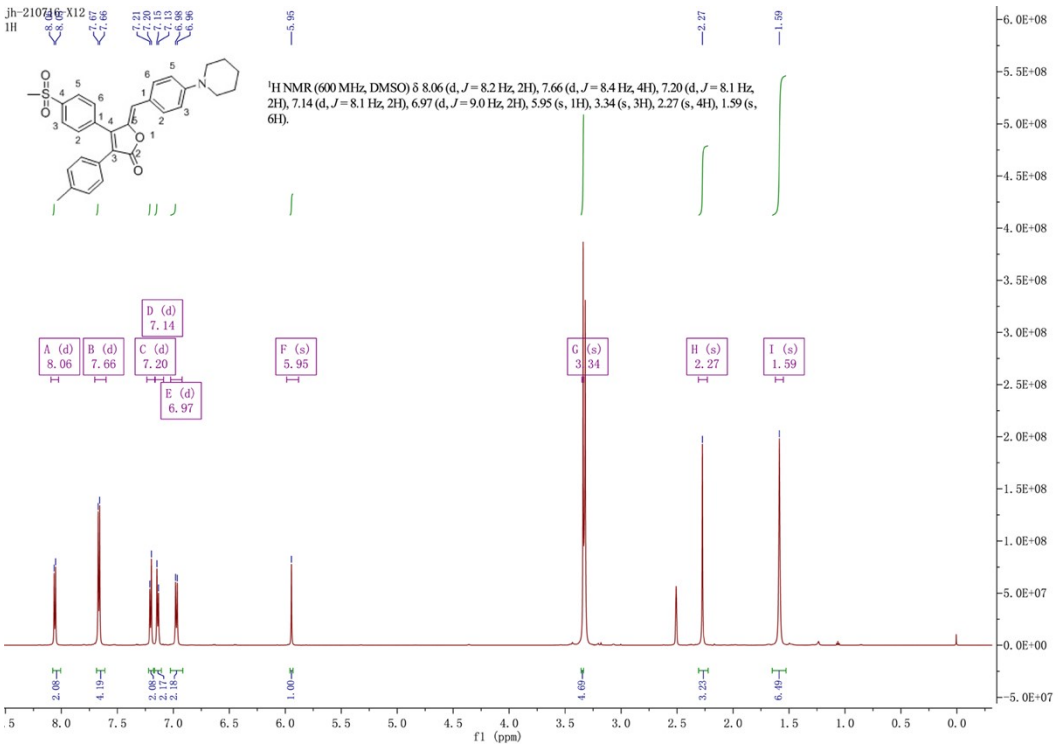

Figure S19. ^{1}H NMR spectrum of **W7** in DMSO-d_6 (600 MHz, 298K).

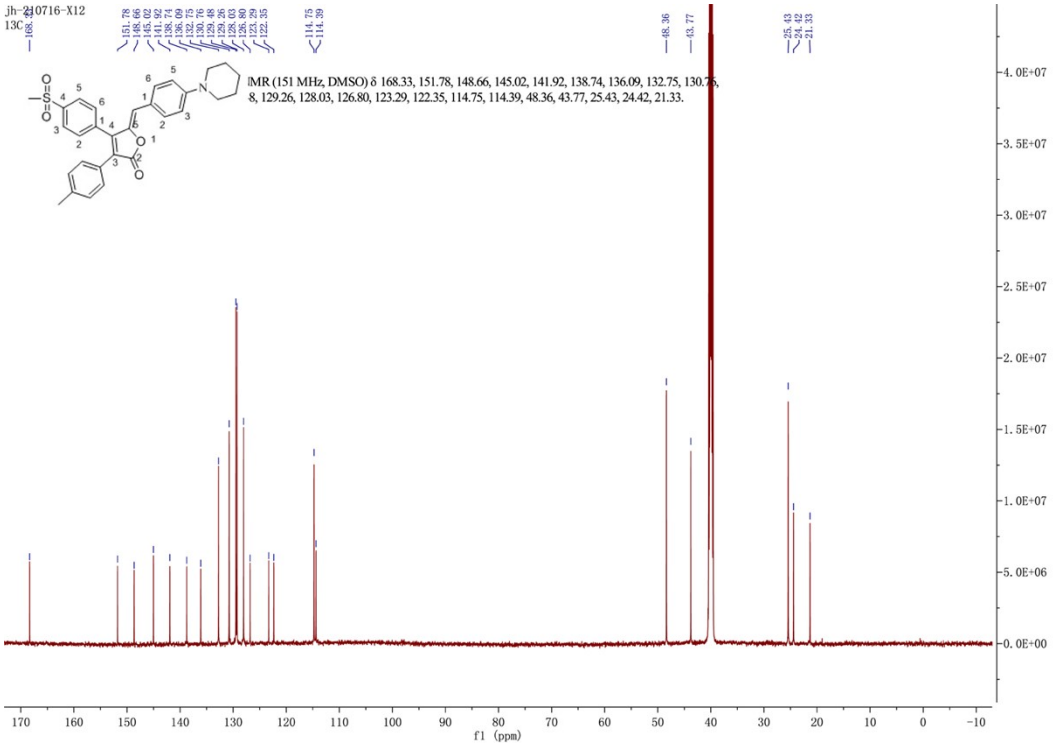

Figure S20. ^{13}C NMR spectrum of **W7** in DMSO-d_6 (151 MHz, 298K).

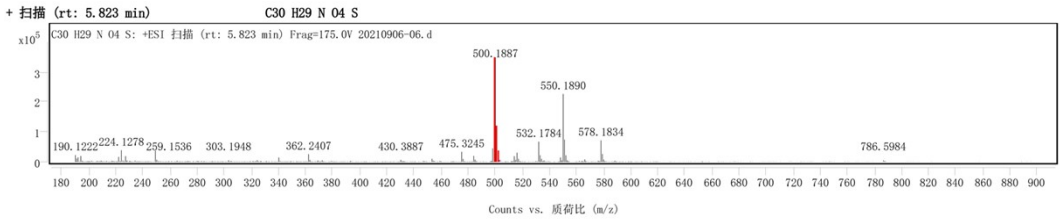

Figure S21. HRMS spectrum of **W7**

Solvatochromism of W1, W4 and W6

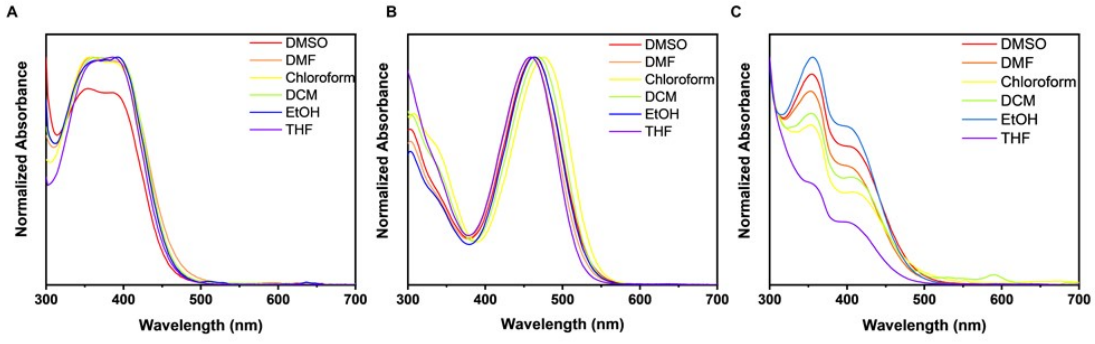

Figure S22. Normalized absorption of compounds (A) **W1**, (B) **W4** and (C) **W6** in various solvents at the concentration of 50 μM, such as DMSO, DMF, chloroform, DCM, EtOH, THF, respectively.

Table S1. The photophysical data of **W1**, **W4** and **W6** in different solvents

compounds	Solvents	λ_{abs} (nm)[a]	λ_{em} (nm)[b]	Δv (cm^{-1})[c]	Stokes shifts (nm)[d]
W1	chloroform	389	600	9040	211
	DCM	392	614	9224	222
	THF	354	620	12120	266
	EtOH	386	646	10427	260
	DMF	356	656	12846	300
	DMSO	358	682	13270	324
W4	chloroform	476	624	4983	148
	DCM	469	644	5894	175
	THF	458	626	5860	168
	EtOH	464	656	6308	192
	DMF	458	676	7041	218
	DMSO	462	690	7152	228
W6	chloroform	352	610	12016	258
	DCM	354	630	12376	276
	THF	354	628	12325	274
	EtOH	356	654	12799	298
	DMF	352	674	13572	322
	DMSO	354	690	13756	336

[a] Absorption maxima, [b] PL intensity maxima, [c] Δv, were calculated using the equation $1/\lambda_{abs}$-$1/\lambda_{em}$, [d] Stokes shifts

Aggregation-induced emission of W1, W4 and W6

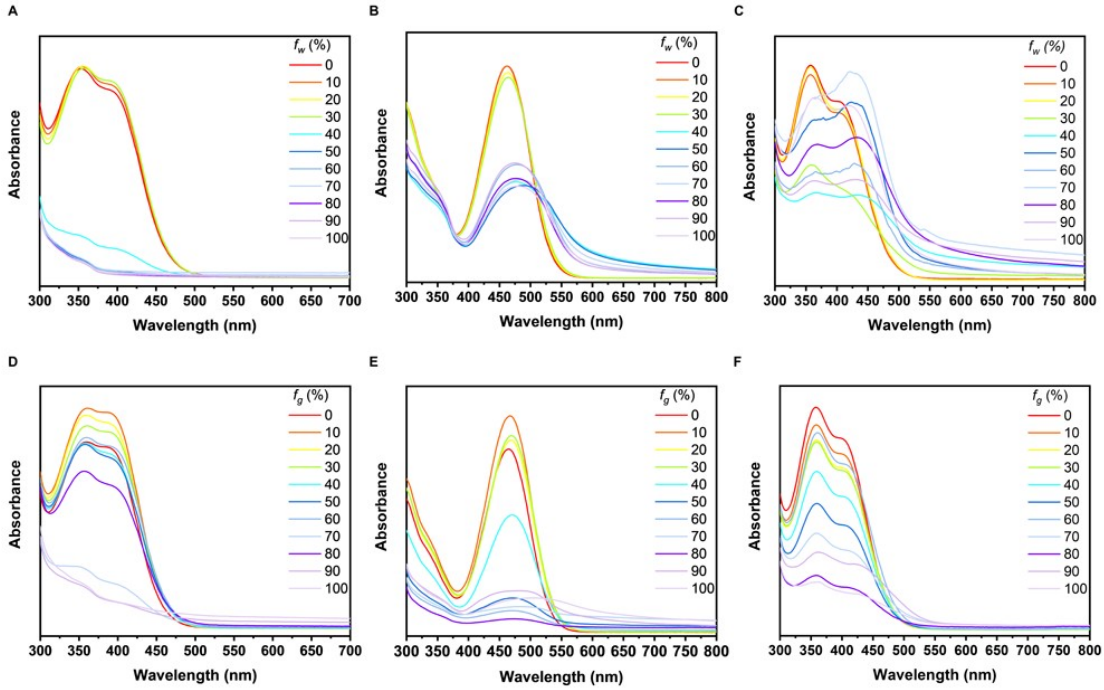

Figure S23. Absorption spectra of (A) **W1**, (B) **W4** and (C) **W6** in DMSO/water mixtures with varied f_w. Absorption spectra of (D) **W1**, (E) **W4** and (F) **W6** ethanol/glycerol mixtures with varied f_g.

Table S2. Solid state fluorescence QY of **W1, W4** and **W6**

compounds	QY
W1	39%
W4	5%
W6	49%

The normalized PL intensity of crystals W6R and W6Y

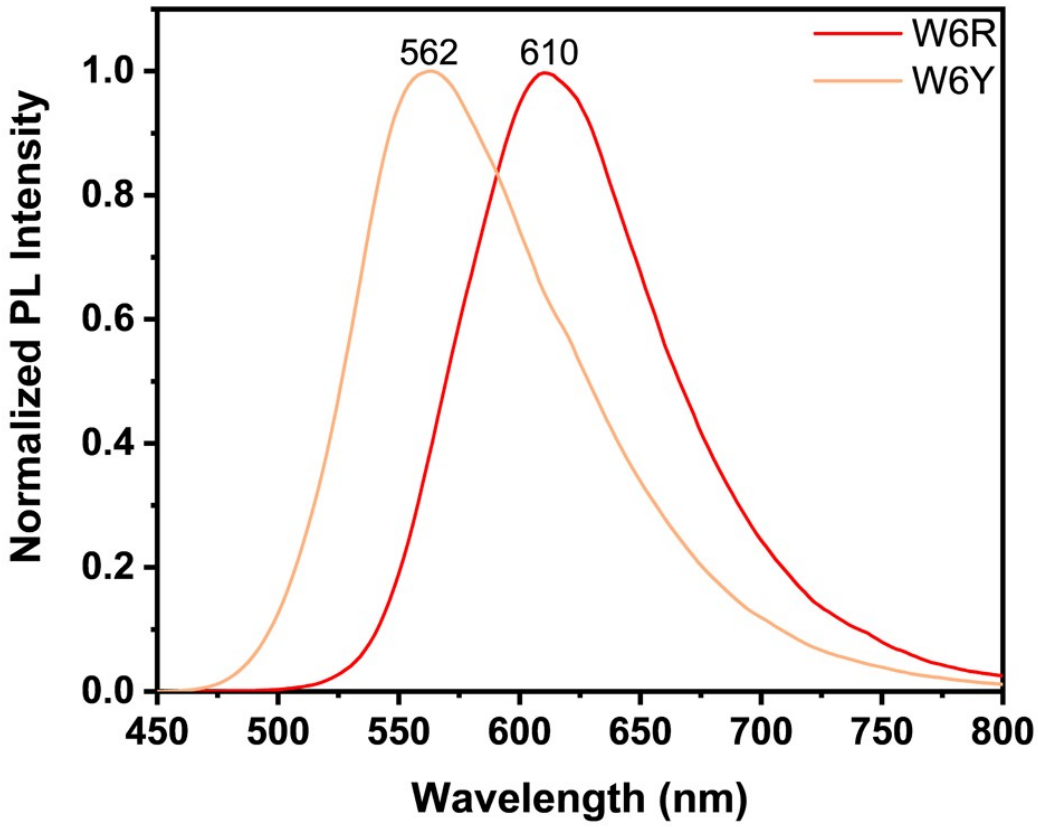

Figure S24. The normalized PL intensity of crystals **W6R** and **W6Y**

Molecular conformation of W1, W6R and W6Y

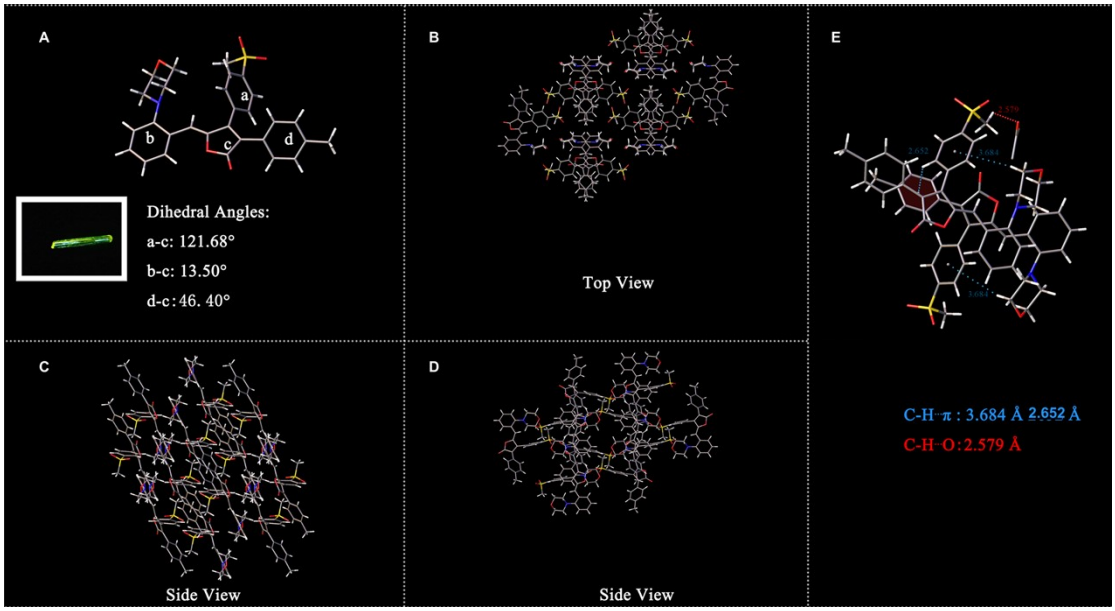

Figure S25. (A-E) Crystal structures. (A) Single crystal strucure and taken photograph of crystal in normal light. (B) Top view and (C,D) side view of packing structure of **W1** crystal, (E) dimer

structure.

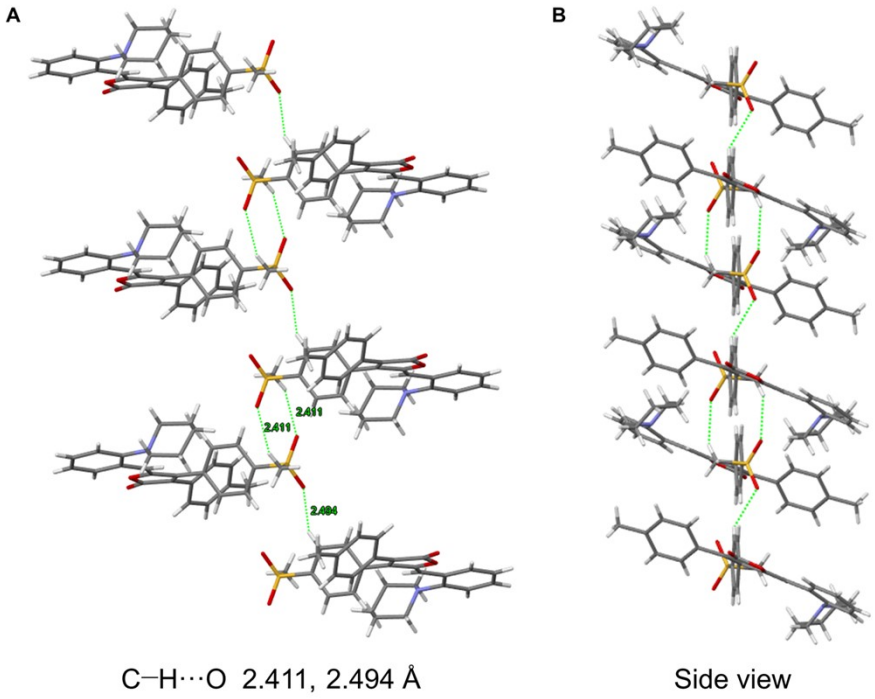

Figure S26. (A) Various intermolecular interactions in crystals of **W6R**. (B) Side view of packing structure of **W6R** crystal.

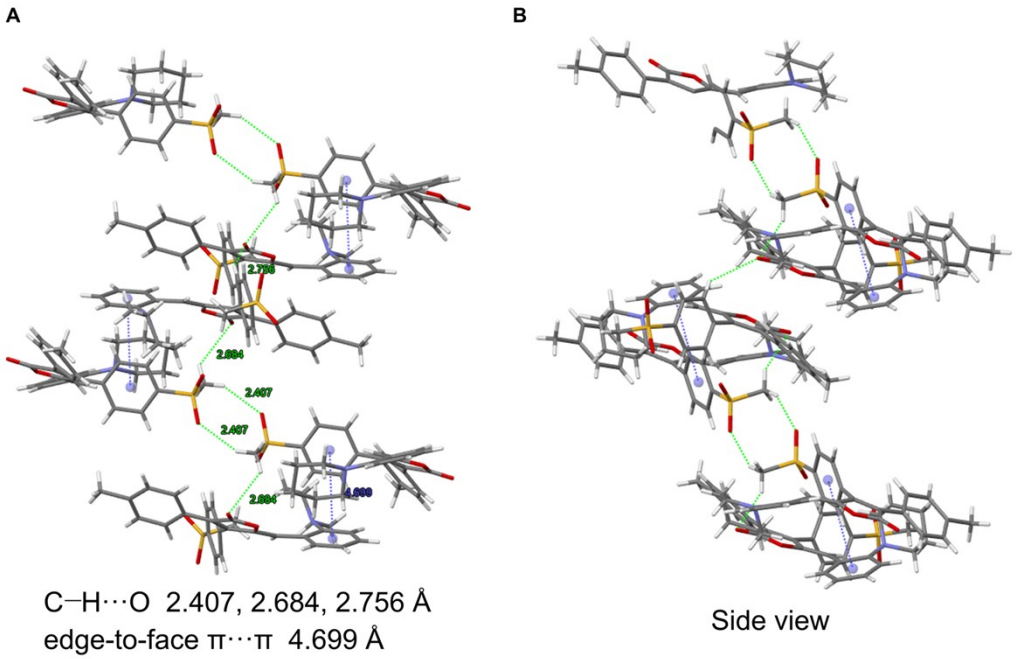

Figure S27. (A) Various intermolecular interactions in crystals of **W6Y**. (B) Side view of packing structure of **W6Y** crystal.

The ORTEP plot of W6R and W6Y

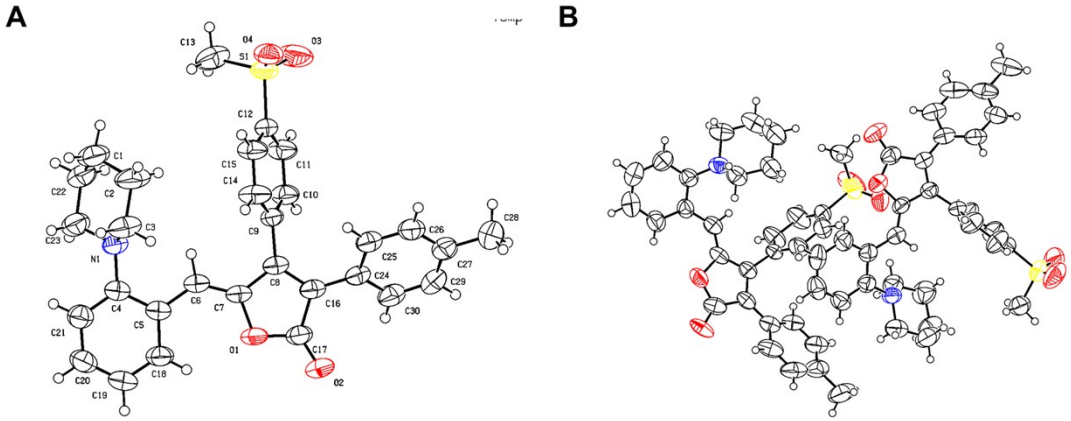

Figure S28. The ORTEP plot of (A) **W6R** and (B) **W6Y**.

Table S3. Crystal data and structure refinement for **W1**.

Identification code	X1
Empirical formula	$C_{29}H_{27}NO_5S$
Formula weight	559.65
Temperature/K	150.01
Crystal system	monoclinic
Space group	$P2_1/c$
a/Å	13.478(3)
b/Å	21.218(4)
c/Å	10.7645(18)
α/°	90
β/°	112.505(6)
γ/°	90
Volume/Å^3	2844.0(10)
Z	4
ρ_{calc}g/cm^3	1.307
μ/mm^{-1}	0.160
F(000)	1184.0
Crystal size/mm^3	0.5 × 0.1 × 0.1
Radiation	MoKα (λ = 0.71073)
2Θ range for data collection/°	4.524 to 54.206
Index ranges	-17 ≤ h ≤ 17, -27 ≤ k ≤ 27, -13 ≤ l ≤ 13
Reflections collected	51550
Independent reflections	6276 [R_{int} = 0.3675, R_{sigma} = 0.1960]
Data/restraints/parameters	6276/5/353
Goodness-of-fit on F^2	1.021
Final R indexes [I>=2σ (I)]	R_1 = 0.0898, wR_2 = 0.1496
Final R indexes [all data]	R_1 = 0.2198, wR_2 = 0.2025
Largest diff. peak/hole / e Å^{-3}	0.39/-0.31

Table S4. Crystal data and structure refinement for **W6R**.

Identification code	mo_X11R_0m_a
Empirical formula	$C_{30}H_{29}NO_4S$
Formula weight	499.60
Temperature/K	299(2)
Crystal system	triclinic
Space group	P-1
a/Å	9.9460(6)
b/Å	12.0390(7)
c/Å	13.2743(8)
α/°	104.081(3)
β/°	103.545(3)
γ/°	113.710(3)
Volume/Å^3	1309.20(14)
Z	2
ρ_{calc}g/cm^3	1.267
μ/mm^{-1}	0.160
F(000)	528.0
Crystal size/mm^3	0.2 × 0.1 × 0.1
Radiation	MoKα (λ = 0.71073)
2Θ range for data collection/°	4.522 to 55.076
Index ranges	-12 ≤ h ≤ 12, -15 ≤ k ≤ 15, -17 ≤ l ≤ 17
Reflections collected	41761
Independent reflections	5999 [R_{int} = 0.0908, R_{sigma} = 0.0520]
Data/restraints/parameters	5999/0/327
Goodness-of-fit on F^2	1.127
Final R indexes [I>=2σ (I)]	R_1 = 0.0606, wR_2 = 0.1675
Final R indexes [all data]	R_1 = 0.1060, wR_2 = 0.2004
Largest diff. peak/hole / e Å^{-3}	0.30/-0.44

Table S5. Crystal data and structure refinement for **W6Y**.

Identification code	mo_X11Y_0ma
Empirical formula	C30H29NO4S
Formula weight	999.20
Temperature/K	299.03
Crystal system	triclinic
Space group	P-1
a/Å	13.4521(16)
b/Å	14.1057(17)
c/Å	14.1605(17)
α/°	90
β/°	90
γ/°	92.405(4)
Volume/Å3	2684.6(6)
Z	2
ρcalcg/cm3	1.236
μ/mm 1	0.156
F(000)	1056.0
Crystal size/mm3	0.3 × 0.2 × 0.1
Radiation	MoKα (λ = 0.71073)
2Θ range for data collection/°	5.782 to 55.032
Index ranges	-17 ≤ h ≤ 17, -18 ≤ k ≤ 18, -18 ≤ l ≤ 18
Reflections collected	36815
Independent reflections	12259 [Rint = 0.2392, Rsigma = 0.2818]
Data/restraints/parameters	12259/0/653
Goodness-of-fit on F2	0.958
Final R indexes [I>=2σ (I)]	R1 = 0.0941, wR2 = 0.1525
Final R indexes [all data]	R1 = 0.3417, wR2 = 0.2424
Largest diff. peak/hole / e Å-3	0.21/-0.22

Mechanochromic luminescence of W4 and W6

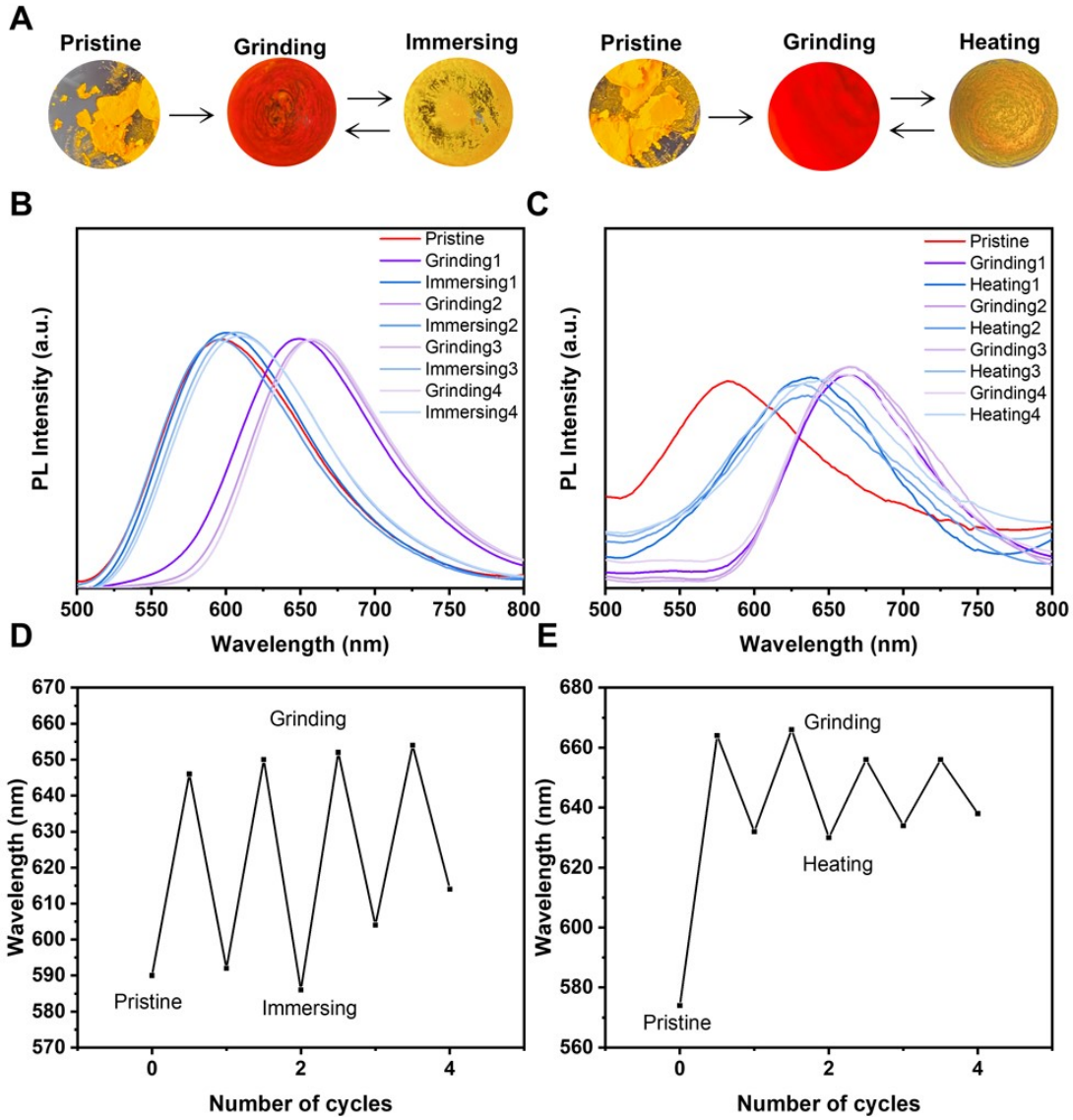

Figure S29. (A) The photographs of **W4** were taken under a 365 nm with hand-held UV lamp at different states. Normalized PL spectra of **W4** at (B) grinding-immersing and (C) grinding-heating process. The process of (D) grinding-immersing treatment and (E) grinding-heating treatment by 4 cycles.

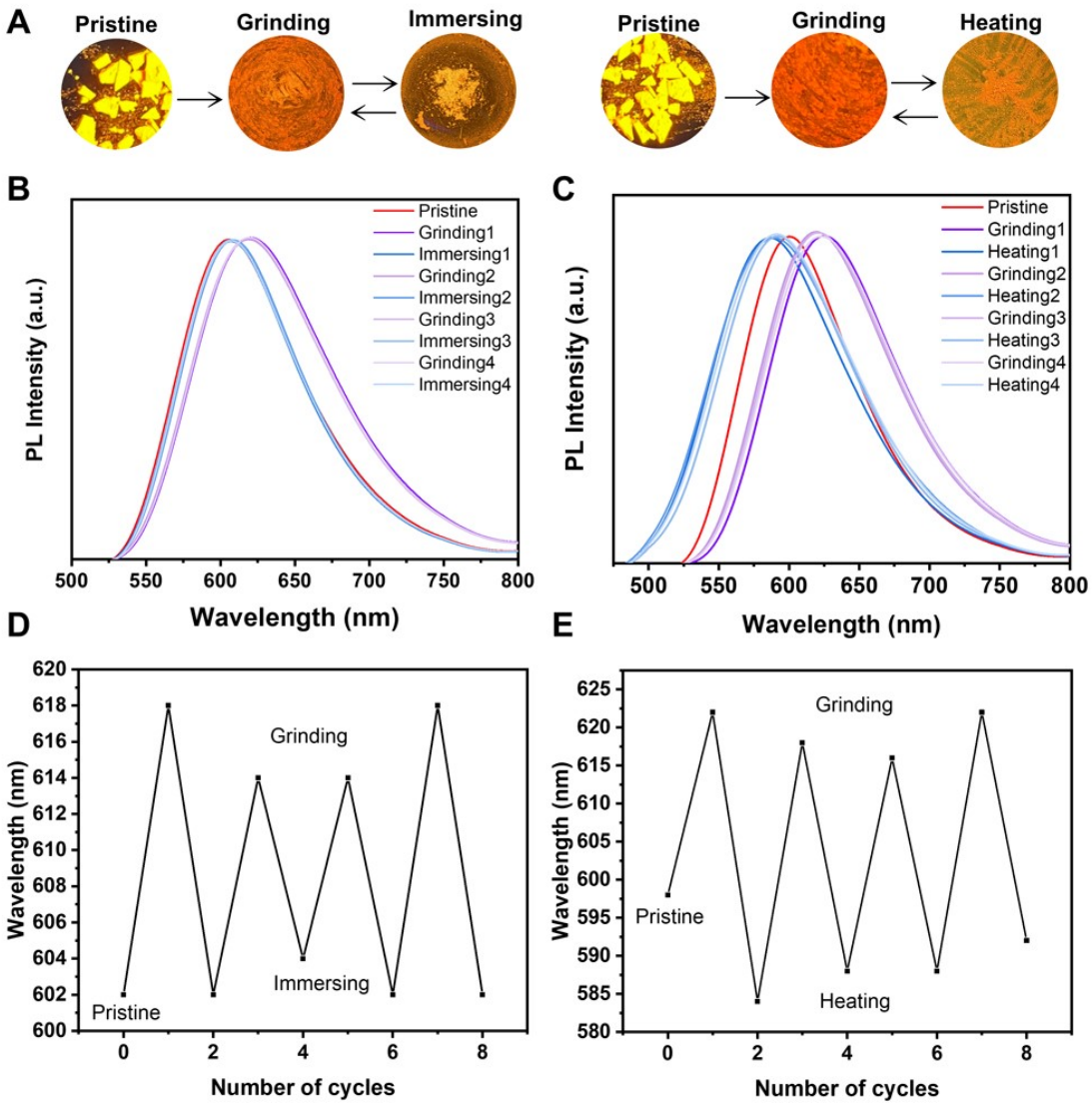

Figure S30. (A) The photographs of **W6** were taken under a 365 nm with hand-held UV lamp at different states. Normalized PL spectra of **W6** at (B) grinding-immersing and (C) grinding-heating process. The process of (D) grinding-immersing treatment and (E) grinding-heating treatment by 4 cycles.

Differential scanning calorimetry of W1 and W6

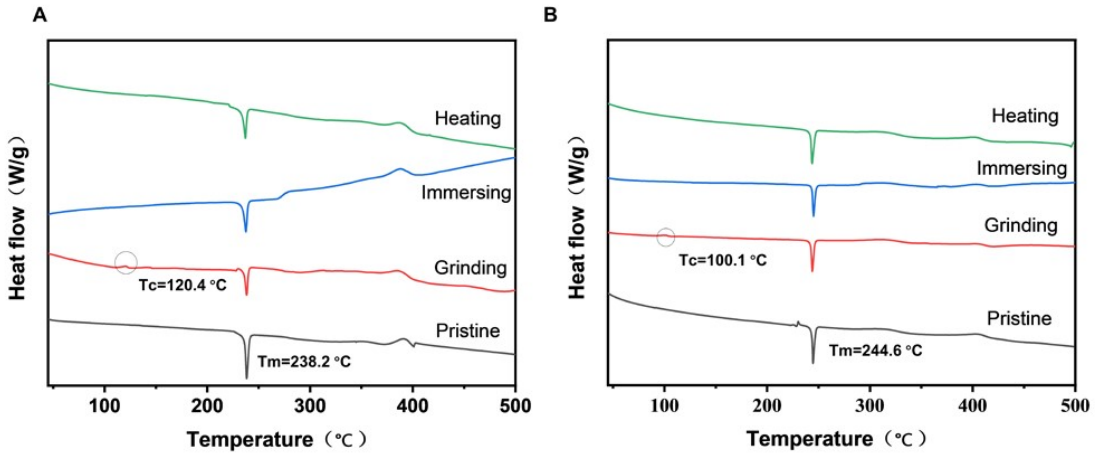

Figure S31. (A) DSC of **W1** in different states: pristine (black line), grinding (red line), immersing with acetone (blue line) and heating (green line). (B) DSC of **W6** in different states: pristine (black line), grinding (red line) immersing with acetone (blue line) and heating (green line).

Sensing properties toward protonic acids of W6

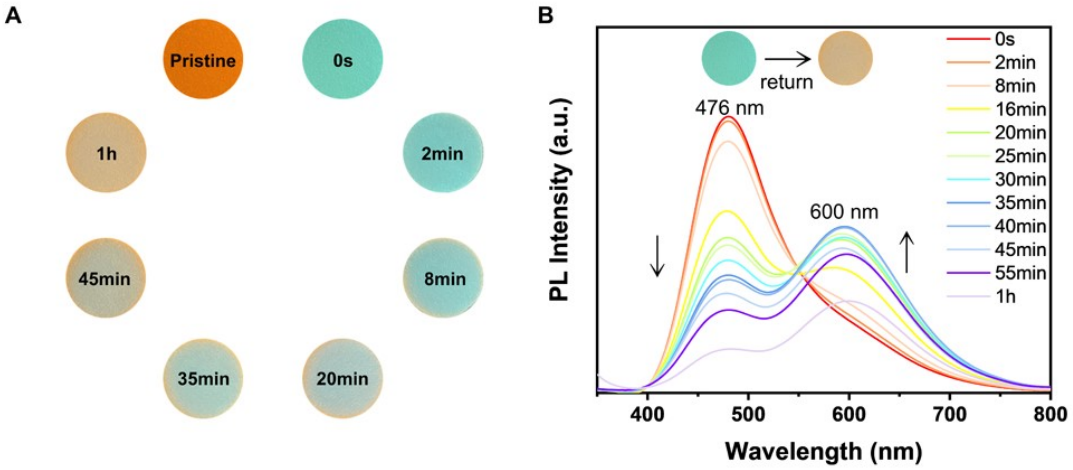

Figure S32. (A) The color change process of **W6** (500 μM) in DCM solvent coated on filter paper with gradually decrease of TFA concentration. (B) spectra of **W6** (500 μM) in DCM solvent coated on filter paper with gradually decrease of TFA concentration and the color change process on filter paper taken under a 365 nm hand-held UV lamp showed in the inset.

Vapochromism of W1

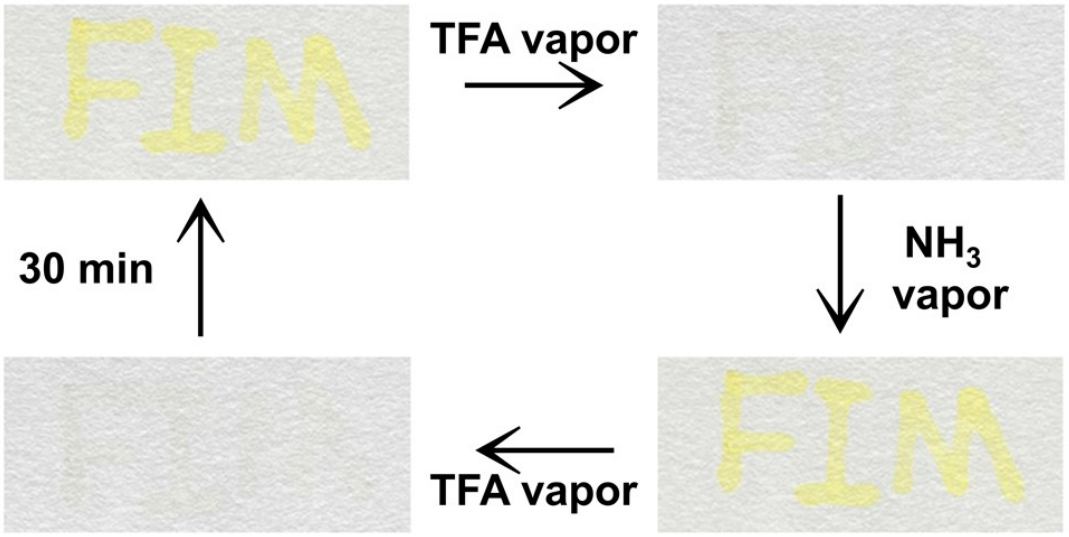

Figure S33. Photographs of filter papers coated with **W1** (10 mM) in DCM solution under different conditions.